STUDY OF THE INFLUENCE OF HEAT SINK GEOMETRIC PARAMETERS ON NATURAL CONVECTION USING ANALYSIS OF EXPERIMENTAL TESTS AND OpenFOAM SIMULATION

Vilson Altair da Silva, altairwayne@gmail.com
Lorenzo Alfonso Caliari de Neves Gomes, gomeslorenzo@gmail.com
Ana Lúcia Fernandes de Lima e Silva, alfsilva@unifei.edu.br
Sandro Metrevelle Marcondes de Lima e Silva, metrevel@unifei.edu.br

Heat Transfer Laboratory – LabTC, Institute of Mechanical Engineering – IEM, Federal University of Itajubá – UNIFEI, Campus Prof. José Rodrigues Seabra, Av. BPS, 1303, 37500-903, Itajubá, MG, Brazil.

Abstract. *The steady state heat transfer by natural convection in heat sinks with rectangular fins positioned vertically and horizontally was studied in this work. The heat transfer by radiation, and an almost uniform temperature in the heat sinks was also considered. This second condition allowed the use of thermocouples only in the center of the heat sink. Twelve heat sinks were designed to study how their geometric parameters such as height, spacing and thickness of the fins, influence the heat transfer by free convection. In addition, in this work, two correlations for heat transfer by free convection using the dimensionless parameters Nusselt and Rayleigh are tested. These correlations were obtained using the results for the 12 heat sinks over a temperature range between 20 °C and 100 °C. Furthermore studies were done to identify which of the 12 evaluated heat sink managed to remove the greatest amount of heat for a given temperature range. The results were compared with results obtained from empirical correlations found in the literature and with a simulation done using open source CFD software OpenFOAM (Open Field Operation and Manipulation) was used to solve the three-dimensional equations of continuity, momentum and energy. This computational simulation uses the PIMPLE solution algorithm for the pressure-velocity coupling and the Finite Volume Method for the discretization of the governing equations. The temperature, velocity and vorticity fields were numerically obtained.*

Keywords*: Heat sinks, Free Convection, Rectangular Fins, Empirical Correlation, Heat Transfer Coefficient, OpenFOAM, Numerical Methods.*

1. NOMENCLATURE

A	m²	Area
b	mm	Fin base Thickness
c_p	J/Kg.K	Specific Heat
ct	-	Cross fin section
$\vec{g}$	m/s²	Vector Acceleration of Gravity
h	W/m.K	Local Heat Transfer Coefficient by Free Convection
$\bar{h}$	W/m.K	Medium Heat Transfer Coefficient by Free Convection
H	m	Fin Height
(H&R)	-	Harahap and Rudianto (2005) [6]
k	W/m.K	Thermal Conductivity
L	m	Heat sink lenght
n	-	Number of fin in Heat sink
Nu	-	Nusselt Number
s	mm	Fin Spacing
t	s	Time
t_w	mm	Thickness
T	K	Temperature
W	m	Fin Width

Special characters

α	m²/s	Thermal Diffusivity
Δ	-	Difference
μ	Pa.s	Dynamics Viscosity
ρ	kg/m³	Specific Mass
∂	-	Differential Operator
∇^2	m⁻²	Laplacian Operator

Subscripts

x	-	Cartesian coordinate
y	-	Cartesian coordinate
z	-	Cartesian coordinate
0	-	Environmental
1	-	Thermocouple Position and Name
2	-	Thermocouple Position and Name
3	-	Thermocouple Position and Name
4	-	Thermocouple Position and Name
5	-	Thermocouple Position and Name
∞	-	Environment

2. INTRODUCTION

A fin is an extended surface from an area where a high heat transfer with the environment is desired. A set of fins is called heat sink. The larger the area of a heat sink, the higher the heat transfer rate. Heat sinks are used in several pieces of equipment that may generate heat and have little space to dissipate heat as motors, transformers, heat exchangers and microprocessors. Heat sinks have been widely studied in order to make better heat transfer rate and in smaller areas without losing their performance.

Natural convection is usually used because it presents high reliability and lower cost and does not use energy. The choice of a heat sink considers the rate of heat dissipated. This rate can be calculated by knowing the average heat

transfer coefficient by convection, $\bar{h}$, which is a property that depends on the fluid flow conditions and the geometry of the surface. The values of $\bar{h}$ can be found by resorting to experiments, numerical solutions and empirical correlations.

Several heat sinks were tested by Silva *et al.* (2015) and two empirical correlations were proposed. These correlations were performed using the software LABfit that is used to obtain an equation from a few experimental points. Using these correlations to obtain values for the *Nusselt Number* the authors can calculate the heat transfer coefficient by convection $\bar{h}$. But Silva *et al.* (2015) used effective length rather than a characteristic length, and because of this their correlation does not approach Nusselt values using a characteristic length its calculation. A correction for this problem is showed in this work.

Tari and Mehrtash (2013) studied the heat sinks in different positions by varying their angles from horizontal to vertical and downwards. This study focused on numerical simulations and on investigation about *Nusselt* and *Rayleigh Numbers*. The purpose was to propose correlations for *Rayleigh Number* by using the numerical simulations for vertical heat sinks and different angles by using the cosine as an adjustment parameter.

Using heat sinks vertically positioned, Kim *et al.* (2013) studied the characteristics of the outflow and the heat transfer with the help of the software FLUENT ®. The authors concluded that optimization of the space between fins do not depend on the height, however, it depends on the length, on the difference between the temperature of the heat sink and the environment, and on the fluid properties. The correlation proposed by Kim *et al.* (2013) was considered more accurate and with a wider range than some correlations proposed previously.

To improve the performance of LED lamps heat sinks are widely used, decreasing the heat in these systems. This theme was studied by Shen *et al.* (2014) and their experimental benched was done to tested heat sink in eight different orientations, started in 0º until 180º, ranging 45º with base of the heat sink and fin in vertical and continuing to 225º until 315º with the fins in horizontal. These tests showed that that worst case was that one where the heat sink was in a angle 270º and the cases of 225º and 315º has a performance much better, especially 315º. The computational results revealed the detailed flow fields and temperature fields and were observed that the mismatch between the heat rejection area and natural convection flow and the blockage of the convection flow are the two dominant factors that deteriorate heat dissipation.

The material of the fins must display high thermal conductivity, and in the present work, aluminum 6063-T5 was used. The material of the fin has great influence on the heat transfer rate once it directly affects the temperature distribution along the extended surface. The optimal configuration would occur if the thermal conductivity of the fin was infinite, thus the temperature along the fin would be the same as the base, providing a maximum rate of heat transfer.

In this study, a simulation using openFOAM, was developed to two heat sinks, similar Gomes (2015). The study of these results was done and validated using a comparison with the empirical correlation obtained by Harahap and Rudianto (2005) and other proposed by Silva *et al.* (2015) and for this one is proposed a correction.

3. THEORETICAL BASIS

In this work, the problem studied is a solid plate subjected to heat transfer by conduction and natural convection. Therefore, the equations of conservation of mass, momentum and energy must be solved. These groups of equations were numerically solved by the software OpenFOAM through the solver chtMultiRegionFoam. The modeling of the solid and fluid domains was done in the next two separated sections.

3.1 Modeling the Solid Medium

The heat flux determination in a section of the solid medium is only possible when the temperature gradient along this medium is known. This temperature gradient can be obtained by applying an energy balance in an appropriated differential control volume.

Considering constant thermophysical properties of the heat sink, the energy conservation can be expressed as:

$$\frac{\partial^2 T}{\partial x^2}(x,y,z,t)+\frac{\partial^2 T}{\partial y^2}(x,y,z,t)+\frac{\partial^2 T}{\partial z^2}(x,y,z,t)=\frac{1}{\alpha}\frac{\partial T}{\partial t}(x,y,z,t) \tag{1}$$

Using the right boundary conditions, Eq. (1) can be used to determine the heat distribution in the heat sink. In this work, tree boundary conditions were used. The Dirichlet Condition (or first-type) specifies a temperature value; the Neumann Condition (or second-type) considers a heat flux on the heat sink boundary (even if it is a null heat flux, as in an adiabatic or isolated surface) and the Robin Condition (or third-type) which considers the heating or cooling of a surface by convection. Figure 1 shows the heat sink geometry and where the boundary conditions above described were applied and also presents the geometric parameters of the heat sink (*L*, *W*, and *H*). The boundary conditions can be expressed as:

- Constant temperature, T_5, in honey pattern area in Fig. 1 (the bottom of the base of the heat sink);

- Isolated Surface is the surface hatched with vertical lines in Fig. 1 (lateral area of the base of the heat sink);
- Cooling by free convection on surface in dotted area in Fig. 1 (the fins surface and the top of the base of the heat sink);

And the initial condition is:

$$T(x,y,z,0)=T_0 \tag{2}$$

Hereafter are described the equations used to model the fluid medium.

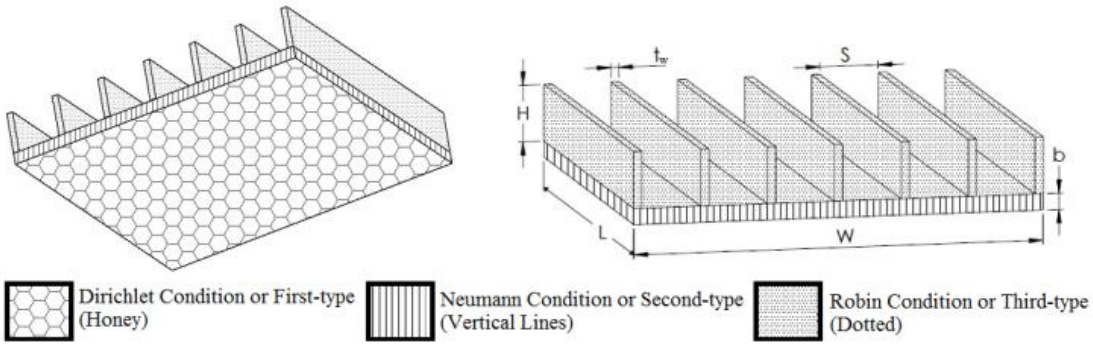

Figure 1. Representation of different domains and the geometric parameters of the heat sink.

3.2 Modeling the Fluid Medium

When considering a compressible flow the mass conservation can be written as:

$$\frac{\partial \rho}{\partial t}+\nabla\cdot\left(\rho\vec{U}\right)=0 \tag{3}$$

Disregarding the viscous dissipation and the internal generation as well as pressure variations, introducing Fourier's law, and considering a constant thermal conductivity the equation is as follows:

$$\frac{\partial T}{\partial t}+u\frac{\partial T}{\partial x}+v\frac{\partial T}{\partial y}+w\frac{\partial T}{\partial z}=\alpha\nabla^2 T \tag{4}$$

By considering the air as a Newtonian fluid and a constant viscosity flow, the momentum equation can be written as the simplified Navier-Stokes equation:

$$\rho\frac{d\vec{U}}{dt}=\rho\,\vec{g}-\vec{\nabla}\,p+\vec{\nabla}\cdot\vec{\vec{\tau}} \tag{5}$$

where τ is the viscous stress tensor.

The button surface of the domain has a condition of heat exchange by free convection with the heat sink and the wood board. Environmental temperature T_1 is imposed to all the lateral surfaces and to the top of the domain (surfaces colored in blue in Fig. 2a). The heating of the fluid happens by heat exchange by free convection with the heat sink. When a closed domain is considered, the boundary conditions for the velocity are null in all surfaces (surfaces colored in blue in Fig. 2a). The pressure was adjusted according to the velocity conditions in all surfaces (surfaces colored in blue in Fig. 2b), whiles a condition of maximum pressure, equal to the atmospheric pressure, is imposed on the top surface (surface colored in red in Fig. 2b).

The domain in this simulation is a 600 mm cube that represents the control volume used as the fluid medium, like that was used by Tari and Mehrtash (2013). The domain is about 43 times bigger than the heat sink height while the length and width are six times the respective dimensions of the heat sink.

The mesh used in all simulations has approximately six millions hexahedral elements. This mesh was chosen after conducting a mesh refinement test, summarized in Table 1. This test was carried out after the steady state was reached.

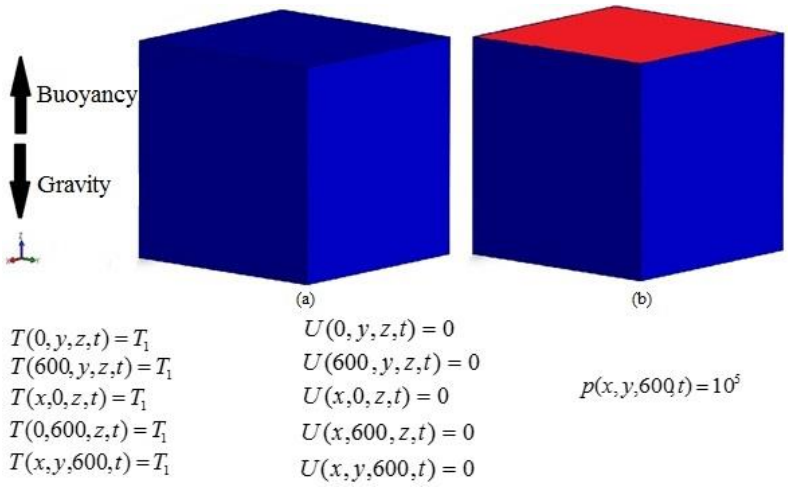

Figure 2. Boundary conditions for temperature and velocity (a) and pressure (b).

Table 1. Mesh refinement test.

Mesh	Elements	Temperature	Simulation Time
I - 220x220xx80	3.5 Millions	310.8 K	24 hours
II - 2060x260x90	6 Millions	315.61 K	80 hours
III - 300x300x90	8 Millions	315.60 K	144 hours

Figure 3 presents three different views of the mesh used.

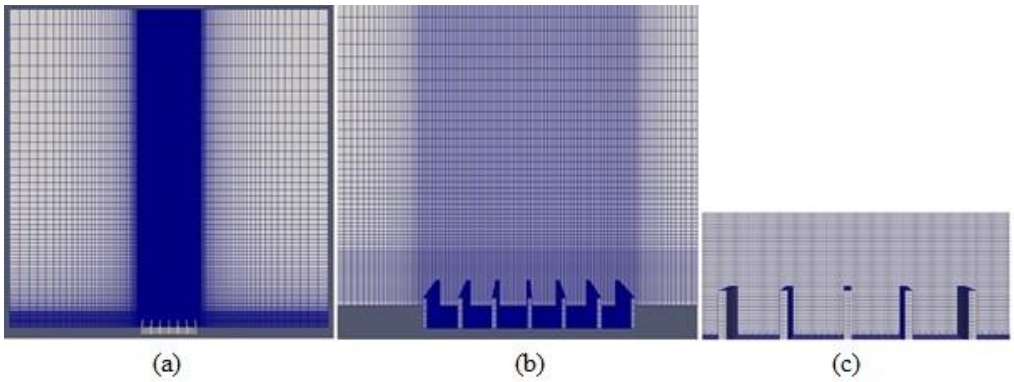

Figure 3. View of the computational mesh. (a) the whole domain, (b) view of the heat sink, and (c) view of the fins.

4. EXPERIMENTAL ASSEMBLY

The experimental apparatus illustrated in Fig. 4a was developed to conduct the tests. The heat sink was assembled on a resistive heater and both placed on a wood support as shown in Fig. 4b. The sidewalls of the support were isolated with glass wool to prevent heat exchange between the support and the heat sink. Additionally, a medium density fiberboard was used to isolate the bottom of the heater to avoid buckling and to keep it in contact with the base of the heat sink. The thermocouples T4 and T5 were fixed by capacitive discharge in the center of the heat sink, T4 on the top and T5 in the base of the central fin. Thermocouple T3 is inserted directly into the heater to reduce the thermal contact resistance, and T2 was used to measure the part of the heat lost by conduction by the MDF (medium density fiber).

The heat sinks were machined from a single 6063-T5 aluminum bar to ensure high thermal conductivity. Figure 1 and Table 2 show the geometric parameters values that made each heat sink different and unique. All these heat sinks were used for experimental tests, but only Heat Sinks 1 and 2 were used for simulations.

The heater used consists of a very thin electrical resistance which can withstand temperatures up to 150º C, already bearing a type T thermocouple inside. This thermocouple is more reliable once it reduces the contact resistance between the heater and the sample and the heater and the MDF isolation. This resistive heater was manufactured by Professor Saulo Güths at Laboratório de Meios Porosos e Propriedades Termofisicas (LMPT) in the Department of Mechanical Engineering at UFSC. This heater was connected to a power source Instrutemp ST-II-305D DC with digital current and voltage display. The twelve heat sinks with different geometrical parameters and the same base were machined from a homogeneous 6063-T5 aluminum bar at the Machining Laboratory at UNIFEI. This aluminum was chosen due to its

wide use in heatsinks and the fact of presenting high thermal conductivity and low density, which are essential characteristics for heat sinks. Another important factor was its affinity with the capacitive discharge welding, a process used to attach the thermocouples directly to the heat sinks.

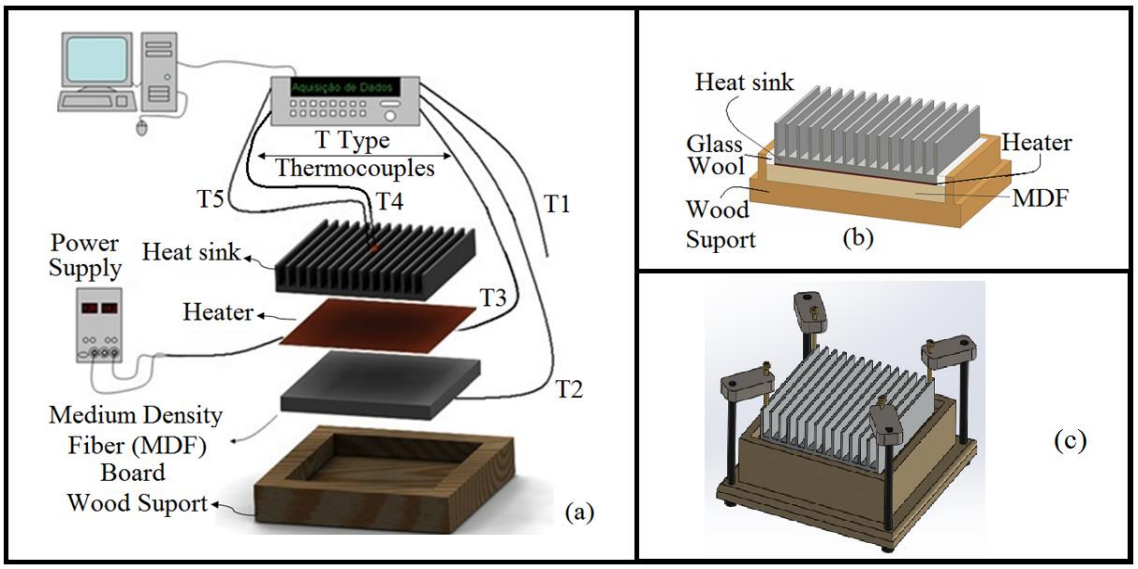

Figure 4. (a) Arrangement of test bench, (b) details of the heat sink and heat sink assembly (c).

Table 2. Dimensions of the Heat sinks.

	S [mm]	t [mm]	H [mm]	L [mm]	W [mm]	b [mm]	n	A_{ct} [m²]
Heatsink	**Fin Spacing**	**Thickness**	**Height**	**Length**	**Width**	**Base Plate Thickness**	**Number of Fins**	**Total Area of Convection**
H1	14,35	2,00	14,00	100,00	100,10	4,00	7	0,0300
H2	5,55	2,00	14,00	100,00	100,15	4,00	14	0,0500
H3	14,35	2,00	20,00	100,00	100,10	4,00	7	0,0386
H4	5,55	2,00	20,00	100,00	100,15	4,00	14	0,0671
H5	14,35	2,00	7,00	100,00	100,10	4,00	7	0,0200
H6	5,55	2,00	7,00	100,00	100,15	4,00	14	0,0300
H7	12,00	4,00	7,00	100,00	100,00	4,00	7	0,0202
H8	3,15	2,00	7,00	100,00	99,85	4,00	20	0,0385
H9	3,15	2,00	20,00	100,00	99,85	4,00	20	0,0916
H10	12,00	4,00	20,00	100,00	99,85	4,00	7	0,0391
H11	3,15	2,00	14,00	100,00	99,85	4,00	20	0,0671
H12	12,00	4,00	14,00	100,00	99,85	4,00	7	0,0304

Five type T thermocouples were used in the assembly. The capacitive discharge welding (Lima *et al.*, 2002) was used because it reduces the contact resistance between the thermocouple and the heat sink. The thermocouples were connected to a data acquisition system, Agilent 34980A, controlled by a computer that filed the temperatures data. The arrangement of the heat sink is shown in Fig. 4c, this assembly reduces heat loss through the bottom surface of the heater because uses pressure to minimize the loss by contact and does not restrict the air flow around the peripheral fins.

5. RESULTS

All the cases were simulated in a computer with a 3.40 GHz CPU and 16.0 GB RAM memory through a virtual machine with a UBUNTU 64 bits operational system. It was also observed that the closed domain did not affect the heat exchange between the heat sink and fluid once the recirculation formed returns to the heat sink with the initial temperature.

For each case analyzed, the same temperatures values used in Silva *et al.* were adopted in the simulation.

Table 3. Temperature values used in the simulations.

	CASE	T_1 [K]	T_5 [K]	ΔT [K]
Heat sink 1	A	295.94	304.30	8.36
	B	296.29	310.92	14.63
	C	295.63	322.07	26.44
	D	297.16	348.32	51.16
	E	295.45	369.26	73.81
Heat sink 2	F	296.84	304.92	8.09
	G	294.77	319.45	24.68
	H	293.55	330.27	36.72
	I	295.68	343.59	47.91
	J	296.07	363.28	67.22

Table 4. Experimental, numerical and analytical temperatures.

	CASE	T_4 experimental	T_4 numeric	T_4 analitical	Deviation
		[K]	[K]	[K]	[%]
Heat sink 1	A	303,86	304,24	304,28	0,13
	B	310,03	310,82	310,89	0,25
	C	320,96	321,85	322,00	0,28
	D	347,39	347,91	348,14	0,15
	E	366,97	368,64	368,97	0,45
Heat sink 2	F	303,38	304,92	304,91	0,51
	G	320,02	319,44	319,41	0,18
	H	331,38	330,25	330,19	0,34
	I	342,47	343,56	343,49	0,32
	J	360,86	363,24	363,12	0,66

In order to validate the numerical results, Tab. 4 presents a comparison between the experimental, numerical and analytical temperatures of the top of the fin after the steady state was reached.

The percent deviations are lower than 0.7% between the numerical and experimental temperatures and it is observed that the analytical and numerical temperatures are close to the experimental temperatures.

A comparison between Heat sink 1 and 2 can be done by analysing Figure 5 where a couple of images shows the temperature fields for cases D and I (Tab 3). These results were chosen due to their approximate power supply values.

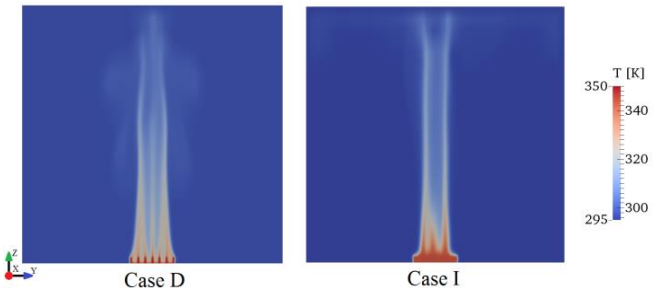

Figure 5. Visual comparison between Case D and Case I.

The differences between the temperature profiles of the fluid on the heat sinks may be observed in Fig. 5. Case I has a more uniform profile in the domain and higher temperatures of the air near the heat sink. In Case D, the temperature profile has more curves over the heat sink which may suggest recirculation.

Figure 6 presents the comparison of the cases for the values of $\bar{h}$ and Nusselt number for Heat sinks 1 and 2. The values obtained numerically and experimentally are close to literature values. Equations (6) and (7) are used by correlations to arrive in the Nusselt number and $\bar{h}$.

Harahap and Rudianto (2005) correlation uses Rayleigh number and calculated in relation to the size of *l*. Thus, Nusselt number is calculated from the equation below:

$$Nu = 0.203 \cdot \left[Ra\left(\frac{nS}{H}\right) \right]^{0.393} \cdot \left(\frac{S}{l}\right)^{0.470} \cdot \left(\frac{H}{l}\right)^{0.870} \cdot \left(\frac{L}{W}\right)^{0.620} \tag{6}$$

where $l = L/2$.

To obtain the experimental values of $\bar{h}$, Newton's cooling law was used, given as:

$$\bar{h} = \frac{q_{pl}}{A_{ct}(T_s - T_\infty)} = \frac{P - q_{iso} - q_{rad}}{A_{ct}(T_s - T_\infty)} \tag{7}$$

where A_{ct} is the total surface area of the heat sink in contact with the fluid, q_{pl} is the difference between the heat transfer rate provided by the heater and lost by conduction, q_{iso}, through the insulator and lost by radiation, q_{rad}, through the heat sink.

To consider only the heater power, the power dissipated by the heater wire that connects to the power supply should be eliminated, so the calculation of the power *P* is done by Eq. (8).

$$P = \frac{(V - R_{fio} I)^2}{R_{aq}} \tag{8}$$

The calculate of q_{iso} and q_{rad} can be done by the Fourier's and Stefan-Boltzmann's Laws, respectively as shown in Eqs.(9) and (10).

$$q_{iso} = k.A\frac{\Delta T_{iso}}{L} = k_{iso}.A\frac{(T_3 - T_2)}{b_p} \tag{9}$$

$$q_{rad} = \varepsilon.\sigma.A_{ct}.(T_S^4 - T_{viz}^4) = \varepsilon.\sigma.A_{ct}.(T_{conv}^4 - T_1^4) \tag{10}$$

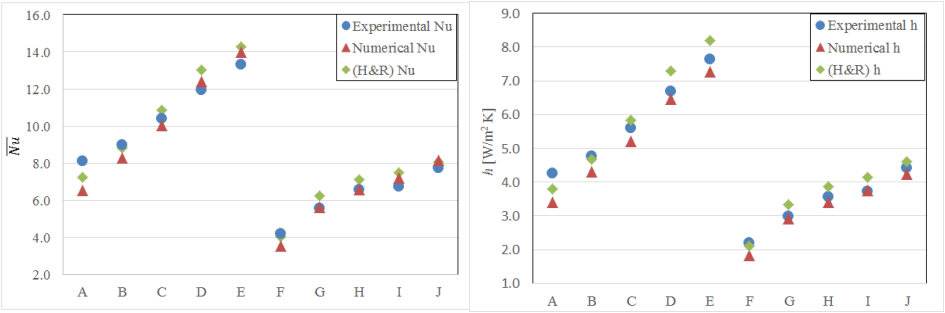

Figure 6. Comparison of experimental, numerical and literature results of Nusselt number and $\bar{h}$ for Heat sinks 1 and 2.

It is evident that Heat sink 1 has greater values for $\bar{h}$ and Nusselt number which means that the energy transferred to the fluid is higher for this case. Heat sink 2 has lower temperatures as shown in Table 4 due to the combined effects of the convection and conduction that occurs in Heat sink 2. So it may be concluded that the combined effects between the convection and conduction are higher in Heat sink 2, even with lower values of $\bar{h}$ and Nusselt number.

The fields of local Nusselt number for cases D (Heat sink 1) and I (Heat sink 2) are shown in Fig. 7.

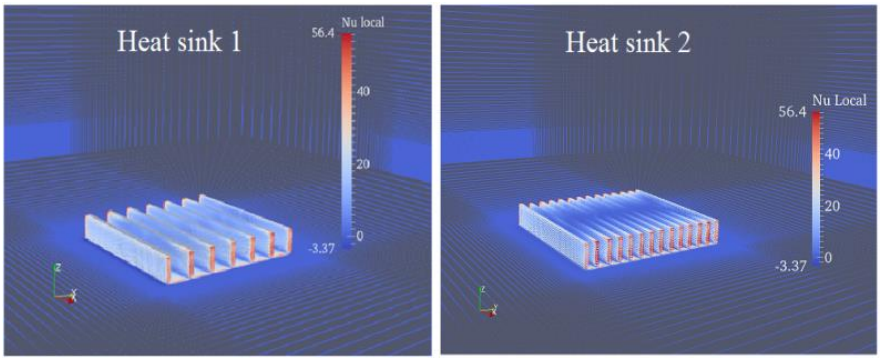

Figure 7. Field of Nusselt Number to Heat sink 1 (Case D) and Heat sink 2 (Case I).

Nusselt number values are higher in the border of the fins close to the spaces where the difference of temperature between the heat sink and the fluid is higher. Consequently, the values of heat exchange by convection and $\bar{h}$ are higher in the red region in Fig. 7.

Figure 8 shows that after 4 seconds of simulation the average Nusselt number becomes constant, what proves one more time that the steady state was reached. Other interesting analysis observed is that the two curves have similar behaviours.

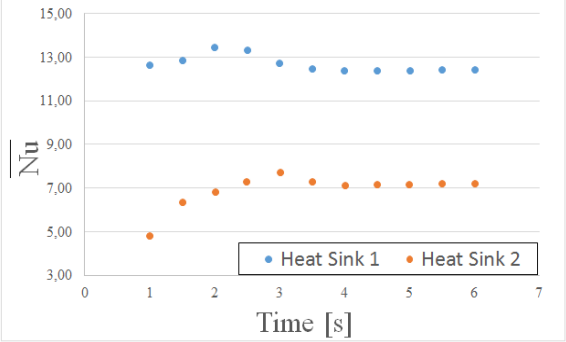

Figure 8. Temporal evolution of the average Nusselt number for Heat sink 1 and 2 in Case D.

Finally, studying the correlation obtained by Silva *et al* (2015), we realize the values obtained to the Nusselt number using the correlation does not approached of the values of others correlations in the literature neither of the simulation of this work. This happen because in the correlation of Silva *et al* (2015) used a effective length to fit its equation. To increase the application of this correlation we propose that the equation is multiplied by a correction factor, how showed in Eq. (11).

$$Nu^* = \frac{l}{L^*} 0{,}086 \cdot Ra^{0{,}266} \cdot \left(S/L\right)^{-0{,}567} \cdot \left(H/L\right)^{-0{,}0169} \cdot \left(t/L\right)^{-1{,}068} \cdot n^{-1{,}580} \tag{11}$$

where l is a characteristic length and L^* is an effective length (L^*=L).

Using the Eq. (11), the results of the simulation and the correlation of Harahap and Rudianto (2005), we build the Fig. 9, that compare each one these values to Nusselt number, axis $\log_{10}(Nu_{calc})$, with the experimental results to Nusselt, axis $\log_{10}(Nu_{exp})$.

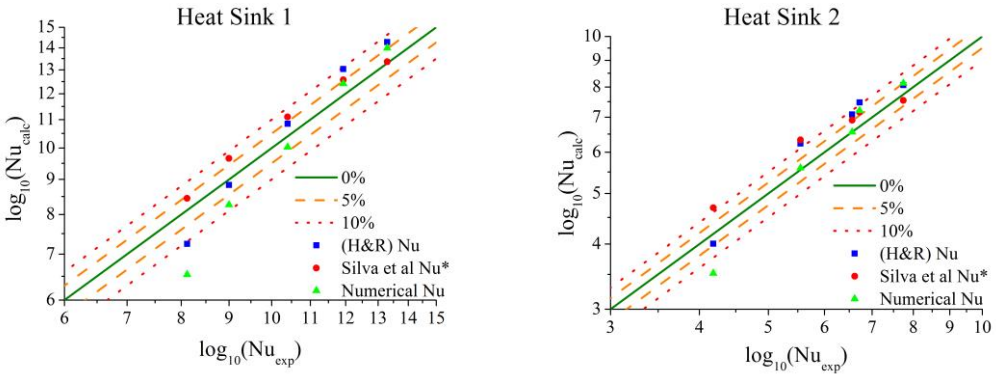

Figure 9. Comparison of Nusselt Numbers Experimental and the calculates Numerical and Experimentally.

The comparison shows that the values of Nusselt are among the line of 10% of the value of the experimental results mostly. One observation done was that the points out the lines of 10% have Rayleigh number close to the extremities proposals by Silva *et al.* (2015) what can explain why this happened. But even with few points going beyond the line of 10% the numerical results and the values finding with the corrected correlation of Silva *et al.* (2015) showed good results and could be validated.

6. CONCLUSION

The thermal fields showed a tendency of raising the fluid, after being heated around the heat sink. In addition, the propagation of the heat is consistent with the movement of the fluid. The recirculation of air in the heat sink, caused by the use of a closed domain, had little influence on the temperature values, since they showed good agreement with average deviations, lower than 0.7%, with experimental and analytical temperature values.

The numerical values of the Nusselt number also showed good agreement when compared with the experimental values and the values obtained by the empirical correlation of Harahap and Rudianto (2005) and Silva *et al.*(2015). The numerical values of $\bar{h}$ also approached the experimental values with an average deviation lower than 8%. When compared to the correlation values, it showed a mean deviation lower than 10%. Noteworthy is the fact that the numerical and experimental values of $\bar{h}$ were closer for the cases with higher temperatures with the lowest deviation of less than 0,6%.

The OpenFOAM software proved to be a reliable tool in the study of heat transfer problems and stands out as an important research tool since it is free and open sourced. Also can be say that the corrected correlation of Silva *et al.* (2015) managed to get a good approximation with the experimental results and with the correlation of Harahap and Rudianto (2005).

7. ACKNOWLEDGEMENTS

The authors would like to thank CNPq, CAPES and FAPEMIG for their financial support.

8. REFERENCES

Gomes, L. A. C. N., 2015. "Study of Heat Transfer by Natural Convection in Heat Sinks Using OpenFOAM", Itajubá, 95p. MSc. Dissertation (in Portuguese), Programa de Pós-graduação em Engenharia Mecânica, Universidade Federal de Itajubá, 2015.

Harahap, F. and Rudianto, E., 2005. "Measurements of steady-state heat dissipation from miniaturized horizontally based straight rectangular fin arrays", *Heat and Mass Transfer*, vol.41, pp. 280-288.

Harahap, F. and Rudianto, E., 2005. "Measurements of steady-state heat dissipation from miniaturized horizontally-based straight rectangular fin arrays", Erratum, *Heat and Mass Transfer*, vol.41, pp. 289-289.

Kim, T. H.; Kim, D. K.; Do, K. H.; 2013. "Correlation for the Fin Nusselt Number of Natural Convective Heat Sinks with Vertically Oriented Plate-Fins", Heat and Mass Transfer, Vol. 49, pp. 413-425.

Lima e Silva, S. M. M., Borges, V. L., Vilarinho, L. O., Scotti, A. e Guimarães, G., 2002. "Desenvolvimento de uma Técnica Experimental para a Determinação do Fluxo de Calor em um Processo de Soldagem TIG (in Portuguese)", 9th Brazilian Congress of Thermal Sciences and Engineering - ENCIT 2002, CDROM, Caxambu, Minas Gerais, Brasil.

Shen, Q., Sun, D., Xu, Y., Jin, T., Zhao, X., 2015. "Orientation effects on Natural Convection Heat Dissipation of Rectangular Fin Heat Sinks Mounted on LEDs" Heat and Mass Transfer, Vol. 75, pp. 462-469.

Silva, V.A., Anselmo, B.C.S., Lima e Silva, A.L.F. and Lima e Silva S.M.M., 2015. "Experimental analysis of the influence of heat sink geometric parameters on natural convection", 23rd ABCM International Congress of Mechanical Engineering, COBEM 2015, Rio de Janeiro, Brazil.

Tari, I. and Mehrtash, M., 2012. "Natural convection heat transfer from inclined plate-fin heat sinks", *Int. J. of Heat and Mass Transfer*, vol. 56, pp. 574-593.

9. RESPONSIBILITY NOTICE

The authors are the only responsible for the printed material included in this paper.